PAPER

# Experimental Validation of Conifer and Broad-Leaf Tree Classification Using High Resolution PolSAR Data above X-Band

**Yoshio YAMAGUCHI**[†a)], ***Fellow***, **Yuto MINETANI**[†], **Maito UMEMURA**[†b)], ***Nonmembers***, ***and*** **Hiroyoshi YAMADA**[†c)], ***Fellow***

**SUMMARY** This paper presents a conifer and broad-leaf tree classification scheme that processes high resolution polarimetric synthetic aperture data above X-band. To validate the proposal, fully polarimetric measurements are conducted in a precisely controlled environment to examine the difference between the scattering mechanisms of conifer and broad-leaf trees at 15 GHz. With 3.75 cm range resolution, scattering matrices of two tree types were measured by a vector network analyzer. Polarimetric analyses using the 4-component scattering power decomposition and alpha-bar angle of eigenvalue decomposition yielded clear distinction between the two tree types. This scheme was also applied to an X-band Pi-SAR2 data set. The results confirm that it is possible to distinguish between tree types using fully polarimetric and high-resolution data above X-band.

***key words:*** *polarimetry, scattering power decomposition, eigenvalue decomposition, conifer, broad-leaf tree*

## 1. Introduction

Forests play an important role in the carbon storage (biomass) and the carbon dynamic cycle. In this regard, forest monitoring by polarimetric SAR (PolSAR) and polarimetric interferometric SAR (PolInSAR) have attracted attention in recent years [1]–[4]. PolSAR information is sensitive to orientation and structural parameters, while PolInSAR information (coherence) is sensitive to spatial variability. The combination of PolSAR and PolInSAR has found to be effective for precise forest mapping and forest-type classification [1]. PolInSAR techniques associated with optimal coherence are now applied to forest type classification and forest height retrieval for accurate biomass estimation [1], [2]. Usually, low observation frequencies are preferred such as L-band or P-band, as they offer deeper penetration into the canopy.

Forests consist of different tree species according to location, varying from tropical rain forest to boreal forest. Typical boreal tree species are broad-leaf and conifer trees. In the middle latitudes, there is some mixture of conifer and broad-leaf trees. There is a need of precise monitoring forest.

This paper shows how to distinguish or classify conifer and broad-leaf trees by polarimetric information present in high frequency SAR. If radar measurements of forests operate above X-band, the penetration depth through the canopy becomes small. The dominant scattering comes from tree canopy at these high frequencies. If the polarimetric scattering mechanisms of these canopies differ, it may be possible to distinguish these tree species from just the polarimetric information.

We have conducted 2-D fully polarimetric measurements of conifer and broad leaf trees at Ku-band in an anechoic chamber to examine the difference of scattering mechanisms. The purpose is to validate the classification possibility of conifer and broad-leaf trees at high frequencies above X band. The previous work [5] showed the possibility in the 2–5.5 GHz range by using entropy-alpha angle (H/$\bar{\alpha}$) decomposition. Following [5], this paper presents the separation results at Ku-band using scattering power decomposition [6] and H/$\bar{\alpha}$ eigenvalue decomposition [7]. A similar classification result was also confirmed by the X-band airborne Pi-SAR2 [8] data set. These experiments support the discrimination capability of conifer and broad-leaf trees by high-resolution PolSAR data.

## 2. Polarimetric Measurement of Conifer and Broad-Leaf Trees

Conifer trees have needle-like leaves. From the high frequency polarimetric scattering point of view, conifer trees can be considered as a cloud of randomly oriented dipoles. In polarimetric measurements, conifer trees generate the cross-polarized $HV$ component at all incidence angles, which yields predominantly volume scattering in the polarimetric scattering power decomposition. On the other hand, the broad-leaf trees have flat leaf surfaces. If the radar incidence angle is less than 45°, radar waves impinge on the leaf surface directly. Surface scattering occurs on the leaves, producing surface scattering power. If the incidence angle becomes larger, radar waves tend to impinge leaf edges and do not induce surface scattering. These scattering and incidence angle characteristics seem significant when the sizes of leaves are comparable with the wavelength. The purpose of our measurements is to examine the different polarimetric responses from these trees at Ku-band.

Using a 4-port vector network-analyzer, full PolSAR measurements were conducted in an anechoic chamber at Niigata University, Japan. The specifications are listed in Table 1. The range resolution is 3.75 cm. Four polarimetric horn antennas were scanned in the azimuth direction along 2.6 m track at 1 cm increments. This data acquisition method

Manuscript received October 10, 2018.
Manuscript revised December 17, 2018.
Manuscript publicized January 9, 2019.

[†]The authors are with Niigata University, Niigata-shi, 950-2181 Japan.
a) E-mail: yamaguch@ie.niigata-u.ac.jp
b) E-mail: umemura@wave.ie.niigata-u.ac.jp
c) E-mail: yamada@ie.niigata-u.ac.jp

DOI: 10.1587/transcom.2018EBP3288

**Table 1** Measurement specifications.

| | |
|---|---|
| Center frequency | 15 GHz |
| Bandwidth | 4 GHz |
| Range resolution | 3.75 cm |
| Azimuth scan interval | 1 cm |
| Scan width | 2.6 m |
| Incidence angle θ | 30°, 45°, 60° |

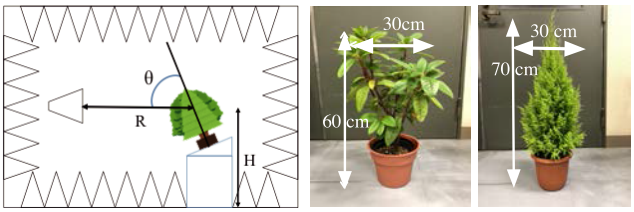


**Fig. 1** Experimental set-up for PolSAR measurement of ornamental broad-leaf and conifer trees.

**Table 2** Range R and height H.

| Incidence angle | R: Broad-leaf | R: Conifer | H |
|---|---|---|---|
| θ = 30° | 2.60 m | 2.51 m | 1.15 m |
| θ = 45° | 2.78 m | 2.70 m | 1.24 m |
| θ = 60° | 3.05 m | 3.00 m | 1.32 m |

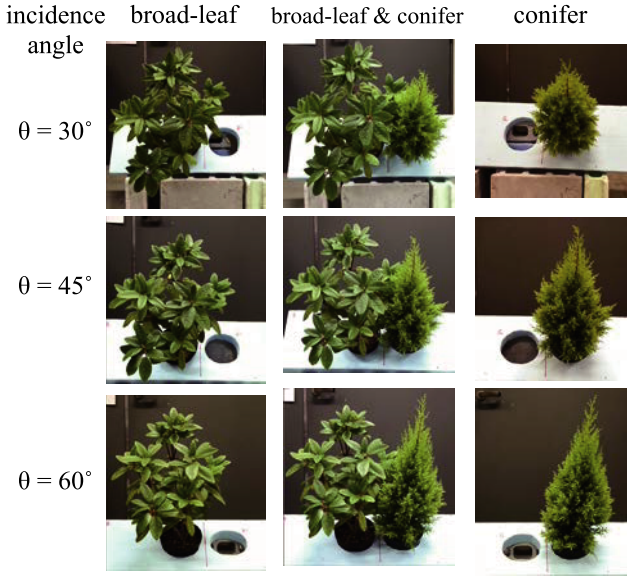


**Fig. 2** Tree arrangements seen from antenna at different incidence angles.

is the same as Stripmap mode of normal SAR system. Small ornamental conifer and broad-leaf tress were used for targets as shown in Fig. 1.

In order to check the incidence angle dependency in the PolSAR scattering, we have inclined trees as shown in Fig. 1 with incidence angles of 30°, 45°, and 60°. The corresponding experimental ranges and heights from the floor are given in Table 2.

Figure 2 shows tree arrangements at different angles. The left column shows a broad leaf tree, the middle is a mixture of both trees, and the right column shows the conifer tree. The upper row is for incidence angle of 30°, the middle row is for 45°, and the lower row is for 60°. These 3 × 3 tree arrangements are used for Figs. 3, 5, 7 and 8 in the next section.

## 3. Analysis Methods

After collecting the PolSAR measurements, scattering matrices for each situation shown in Fig. 2 were obtained. Then we analyzed the data sets using the 4-component scattering power decomposition [6] and alpha-angle [7]; these are well known methods in polarimetric data analysis [9].

### 3.1 Scattering Power Decomposition

First, 4-component scattering power decomposition [6] was applied to the data sets. This method decomposes the total power $TP$ of an imaging window into the surface scattering power $Ps$, the double bounce power $Pd$, the volume scattering power $Pv$, and the helix scattering power $Ph$.

$$\text{Total Power: } TP = Ps + Pd + Pv + Ph \tag{1}$$

These powers are used to create RGB color-coded images with $Pd$ assigned to Red, Green to $Pv$, and Blue to $Ps$. The helix power $Ph$ is assigned to Yellow (1/2 Red and 1/2 Green). The $HV$ component in this study plays the most important role in tree classification. The window size in this analysis was chosen as 2 × 3, with 2 pixels in the range direction and 3 pixels in the azimuth direction. This window size (7.5 cm × 3 cm) was determined considering the tree size and radar resolution.

Figure 3 shows the scattering power decomposition image yielded by the tree arrangement in Fig. 2. The broad-leaf tree exhibits a blue color and conifer tree looks green, from this we can distinguish two tree types by color information. As incidence angle becomes larger (up to 60°), the volume scattering power $Pv$ (Green) increases slightly as a general rule. If the incidence angle becomes even larger, radar waves tend to impinge on the leaf edges and do not induce surface scattering. Due to the high-resolution of the data sets, it is possible to see the details and the scattering properties of tree structures by eye inspection.

If we check the decomposition result quantitatively, the power ratio becomes as shown in Fig. 4. The power ratio of the 4-component scattering powers is displayed for broad-leaf and conifer trees for the case of 30° incidence angles. We confirmed that $Ps$ is dominant in the broad-leaf, whereas $Pv$ is dominant in the conifer tree.

### 3.2 Eigenvalue Decomposition — H/Alpha-Bar Angle

Since the scattering power decomposition image distinguishes broad-leaf and conifer tree by color, it seems that it should be possible to classify them by other polarimetric indexes. We applied the H/alpha-bar classification from the eigenvalue analysis [7] to the same data sets. Since this

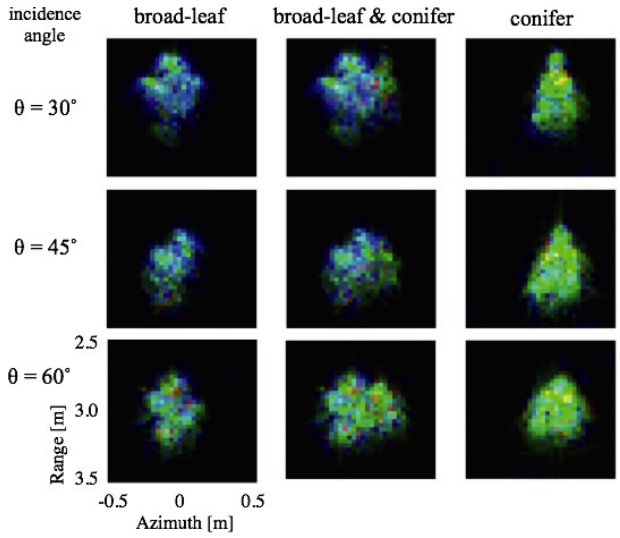


**Fig. 3** Color-coded scattering power decomposition [6] images with Blue corresponding to the surface scattering power $Ps$, Green to the volume scattering power $Pv$, Red to the double bounce scattering power $Pd$, and Yellow to the helix scattering power $Ph$.

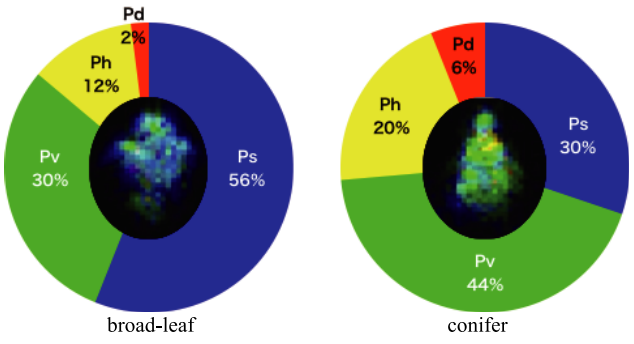


**Fig. 4** Decomposition power ratios.

method is well established, and the most frequently used one in the PolSAR data analysis [9], the details of the method are omitted here. After obtaining the 3 eigenvalues ($\lambda_1$, $\lambda_2$ and $\lambda_3$) of the coherency matrix in an imaging window, the alpha-bar angle $\bar{\alpha}$ is derived as

$$\bar{\alpha} = P_1\alpha_1 + P_2\alpha_2 + P_3\alpha_3 \quad (0^\circ \le \bar{\alpha} \le 90^\circ) \tag{2}$$

where,

$$P_i = \frac{\lambda_i}{\lambda_1 + \lambda_2 + \lambda_3} \quad (i = 1, 2, 3) \tag{3}$$

The value of $\bar{\alpha}$ roughly corresponds to that of flat surface ($\bar{\alpha} = 0^\circ$), dipole ($\bar{\alpha} = 45^\circ$), and dihedral ($\bar{\alpha} = 90^\circ$). The alpha-bar angle represents the polarimetric scattering mechanism.

Figure 5 shows the corresponding results to Fig. 2. We see that conifer trees have large $\bar{\alpha}$ (Red) and broad-leaf trees exhibit small value (Blue). Thus it also seems possible to distinguish these trees by $\bar{\alpha}$.

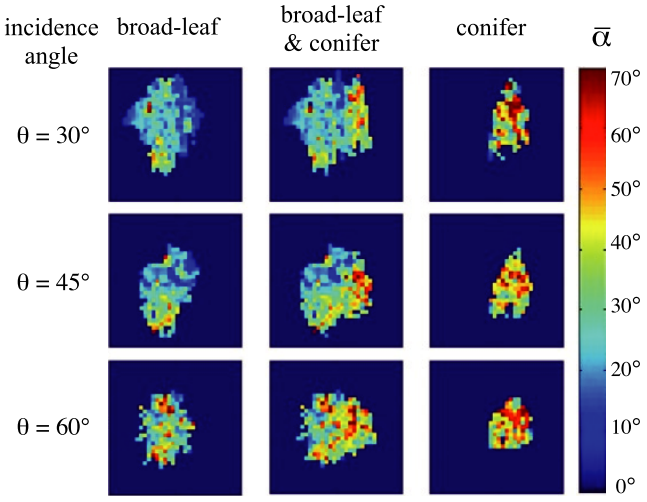


**Fig. 5** Alpha-bar angle of two tree types.

## 4. Classification

Based on the results of Fig. 3 and Fig. 5, it seems possible to classify conifer and broad-leaf trees by a combined use of the scattering powers (especially using the volume scattering power $Pv$) and alpha-bar angle.

Figure 6 shows a simple algorithm for classification. The algorithm, first obtains the scattering powers ($Ps$, $Pd$, $Pv$, and $Ph$) and excludes noise power lower than a threshold ($-45$ dB in this case). The threshold power level is dependent on the instrument and measurement environment. Then the algorithm classifies these trees by alpha-bar angle, where threshold angle is set $\bar{\alpha} = 30^\circ$. This threshold level may be dependent on tree species and on the radar resolution at SAR operating frequency.

Both tree types are clearly distinguished as seen in Fig. 7 when compared to Fig. 2. This indicates the usefulness of the polarimetric information. The classification result arises from both the high-resolution imagery and the nature of the high frequency scattering. If the resolution is coarser, then the dominant scattering will become volumetric for both species. In such a case, it would be difficult to distinguish tree type. If the SAR frequency is lower than C-band, the radar wave will penetrate deeper into trees and will not provide much information on the tree canopy. In such a case, it is also difficult to classify tree type.

In addition to alpha-bar angle classification, it seems possible to execute the same procedure by decomposition powers only. If all processing is carried out by scattering powers, it will be easy and beneficial for the signal processing. In this sense, we tried the next parameter for classification.

$$\text{Power Anisotropy: } PA = \frac{P_s - P_v}{P_s + P_v} \tag{4}$$

This definition is quite simple as shown in the numerator (4). The classification criterion is decided after some trials.

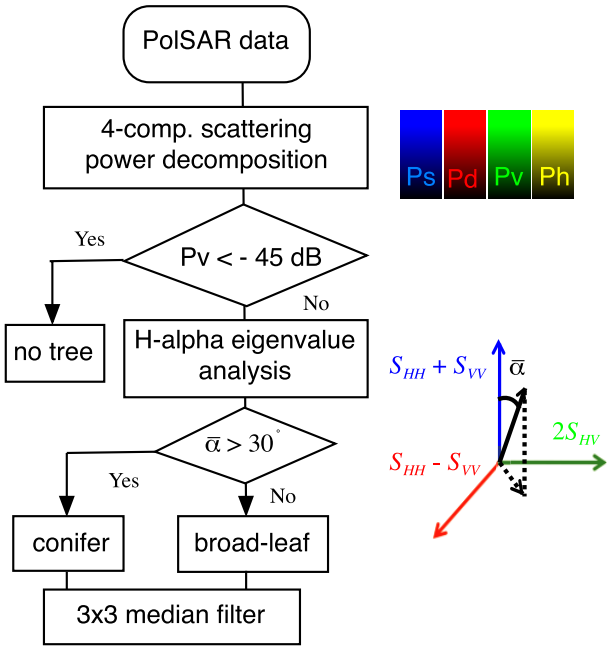


**Fig. 6** Classification algorithm.

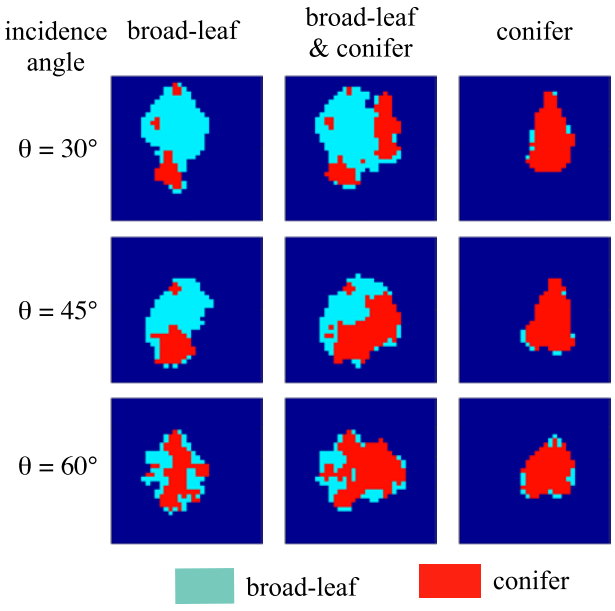


**Fig. 7** Classification result of tree types by alpha-angle.

If $PA < 0.2$ then Conifer.

If $PA > 0.2$ then Broad-leaf.

This rule was applied to the same data set of Fig. 7. The classification results are shown in Fig. 8, which are similar to those in Fig. 7 with blue enhanced slightly. Since both methods provide almost similar results, we can use them by our preference. However, from the theoretical point of view, alpha angle method utilizes full polarimetric information, it would be safer to use alpha-angle method.

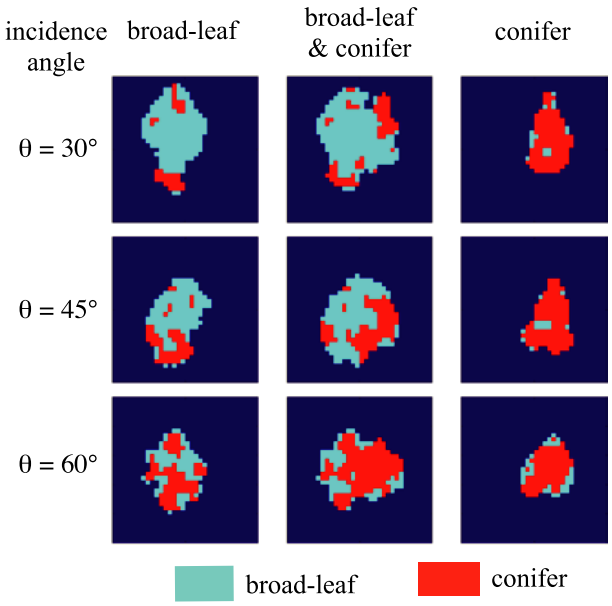


**Fig. 8** Classification result of tree types by power anisotropy.

(a) Whole area of Yoyogi-Park in central Tokyo, Japan.

(b) Street view along a white arrow in Fig. 10.

**Fig. 9** Yoyogi-Park by Google Earth.

## 5. Application to Real Observation Data

The experimental results at Ku-band in the anechoic chamber suggested that polarimetric scattering characteristics play an important role in tree discrimination. The effective parameter seems to be leaf size with respect to wavelength, resolution, and penetration capability. In order to check the

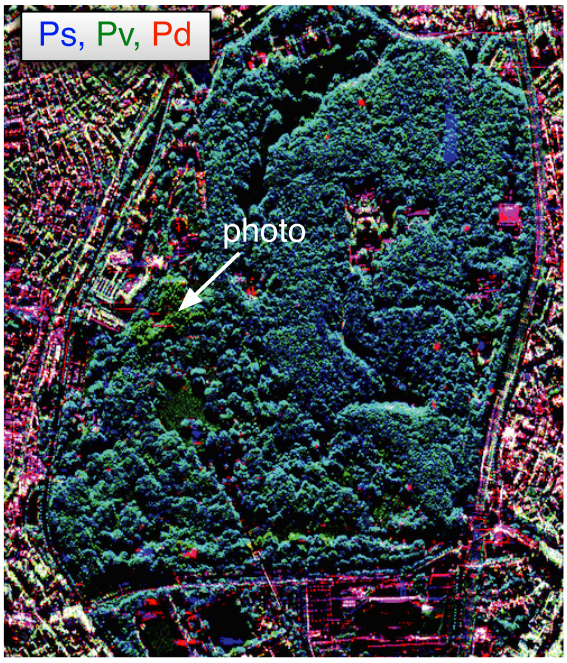


(a) Color-coding: Red(Pd), Green(Pv), Blue(Ps)

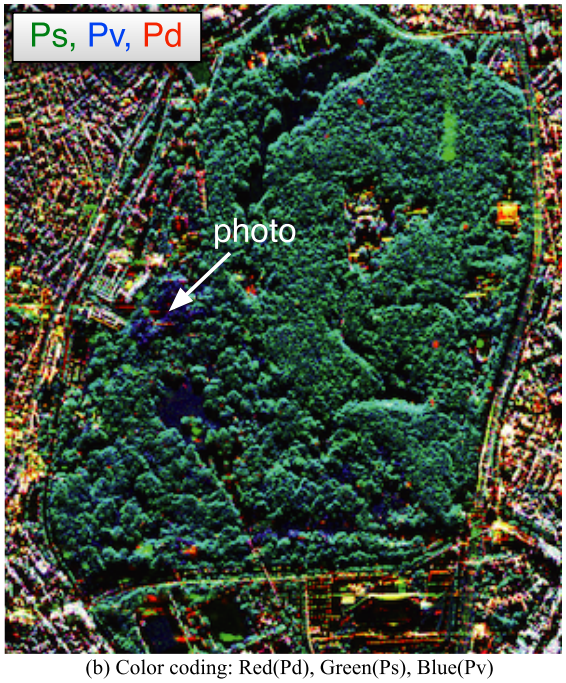


(b) Color coding: Red(Pd), Green(Ps), Blue(Pv)

**Fig. 10** Scattering power decomposition image of Yoyogi-Park, Tokyo on Aug. 26, 2013.

discrimination availability at X-band and the discrimination capability in the real world, we extended the previous analyses to the actual airborne Pi-SAR2 data set, acquired by NICT on Aug. 26, 2013. Pi-SAR2 is a fully polarimetric SAR system with the very high-resolution capability of 30 cm × 30 cm on the ground [8]. The incidence angle was approximately 50 degrees at Yoyogi-Park in Tokyo, Japan. Fig. 9 shows a Google Earth image of Yoyogi-park in central

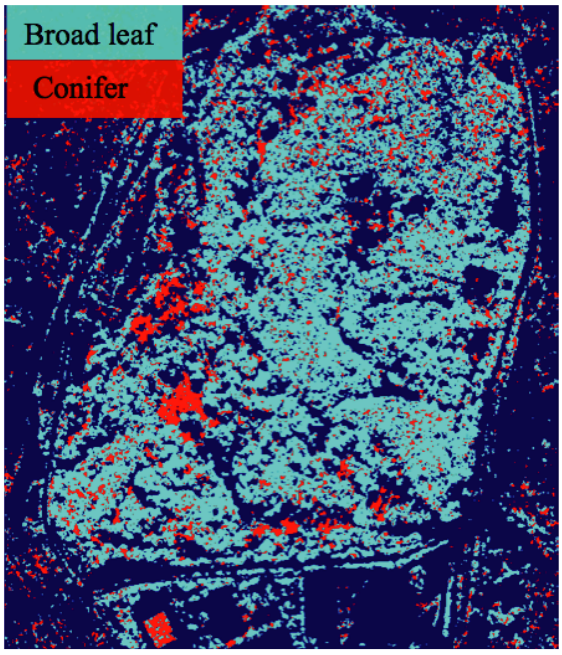


**Fig. 11** Classification of conifer and broad-leaf tree in Yoyogi-Park.

Tokyo, Japan.

First, the scattering power decomposition was performed on the acquired data. The decomposition image is shown in Fig. 10, where two color-coding methods are employed. Figure 10(a) is color-coded with commonly used assignment, i.e., Red for Pd, Green for Pv, and Blue for Ps. On the other hand, Fig. 10(b) is color-coded with Green for Ps and Blue for Pv. The reason to change the color-coding is intuitive recognition of our eyes. Although the same decomposition result is displayed in Fig. 10, it seems easier for our eye to recognize trees with green color as shown in Fig. 10(b). This is based on our knowledge that broad leaves in general have brighter green than conifer leaves.

The image is very vivid and seems easy to interpret. Most of green mixed with blue areas correspond to broad-leaf trees in Fig. 10(b). However, there are some areas colored dark blue indicated by the white arrow. These green areas correspond to the conifer trees shown in Fig. 9(b). Other localized dark blue areas in the lower image were also confirmed as conifer trees by Google Earth image.

Then, based on the decomposition result of Fig. 10, the same classification scheme with $\bar{\alpha} = 40°$ was applied to the data set. The classified image is shown in Fig. 11, where red spots correspond to conifer trees. Other red dots in the whole park are caused by random scattering from complicated structure of trees. The classification result almost agrees with the result of Fig. 10 and Google Earth image. Therefore, the ability to discriminate polarimetrically conifer and broad-leaf trees was demonstrated by the X-band Pi-SAR2 data set. The high-resolution capability and polarimetric information served each other for this discrimination.

## 6. Conclusion

Fully polarimetric SAR measurements in the Ku-band were conducted to discriminate conifer and broad-leaf trees in an anechoic chamber. Scattering power decomposition and alpha-bar angle of eigenvalue analyses provided clear distinction between the two tree types. This scheme was then applied to high-resolution PolSAR data at X-band. We confirmed that discrimination between conifer and broad-leaf trees was possible by processing airborne Pi-SAR images of Yoyogi-Park. Not only by the measurement data in a well-controlled anechoic chamber but also by real-world data acquired with airborne SAR demonstrated that accurate discrimination of conifer and broad-leaf trees was possible. Therefore the initial purpose of the paper was validated.

The discrimination of tree types depends on the scattering characteristics of the tree leaves with respect to size, frequency (wavelength), resolution, and penetration capability. Although these relations are complicated, high-resolution and fully polarimetric data at higher frequencies (Ku- and X-band) will bring interesting results for future forest monitoring.

## Acknowledgments

The authors are grateful to National Institute of Information and Communications Technology (NICT), Japan, for providing Pi-SAR2 data sets for research purpose under contract. We appreciate Dr. Thomas L. Ainsworth and IEICE Editorial Committee for improving English.

### References

[1] J.S. Lee and E. Pottier, Polarimetric Radar Imaging: From Basics to Applications, Ch. 9, CRC Press, 2009. ISBN 9781420054972.
[2] A. Moreira, P. Prats-Iraola, M. Younis, G. Krieger, I. Hajnsek, and K.P. Papathanassiou, "A tutorial on synthetic aperture radar," IEEE Geosci. Remote Sens. Mag. (replaces Newsletter), vol.1, no.1, pp.6–43, March 2013. DOI: 10.1109/MGRS.2013.2248301
[3] Global PALSAR-2/PALSAR/JERS-1 Mosaic and Forest/Non Forest map, http://www.eorc.jaxa.jp/ALOS/en/palsar_fnf/fnf_index.htm, accessed Oct. 1, 2018.
[4] JICA-JAXA Forest Early Warning System in the Tropics, http://www.eorc.jaxa.jp/jjfast/, accessed Oct. 1, 2018.
[5] S. Cloude, J. Fortuny, M.L.-Sanchez, and A.J. Sieber, "Wideband polarimetric radar inversion studies for vegetation layers," IEEE Trans. Geosci. Remote Sens., vol.37, no.5, pp.2430–2441, Sept. 1999. DOI: 10.1109/36.789640
[6] Y. Yamaguchi, T. Moriyama, M. Ishido, and H. Yamada, "Four-component scattering model for polarimetric SAR image decomposition," IEEE Trans. Geosci. Remote Sens., vol.43, no.8, pp.1699–1706, Aug. 2005. DOI: 10.1109/TGRS.2005.852084
[7] S. Cloude and E. Pottier, "An entropy based classification scheme for land applications of polarimetric SAR," IEEE Trans. Geosci. Remote Sens., vol.35, no.1, pp.68–78, Jan. 1997. DOI: 10.1109/36.551935
[8] Pi-SAR2, https://www.nict.go.jp/out-promotion/other/case-studies/itenweb/Pi-sar2.html, accessed Oct. 1, 2018.
[9] PolSAR Pro, https://earth.esa.int/web/polsarpro/home, accessed Oct. 1, 2018.
[10] Y. Yamaguchi, Y. Minetani, and H. Yamada, "Polarimetric response from conifer and broad-leaf tree at Ku-band in anechoic chamber," Electronic Proc. IGARSS 2018, Spain, July 2018.
[11] Y. Yamaguchi, G. Singh, and H. Yamada, "On the model-based scattering power decomposition of fully polarimetric SAR data," Trans. IEICE Commun. (Japanese Edition), vol.J101-B, no.9, pp.638–647, Sept. 2018, DOI: 10.14923/transcomj.2018API0001

**Yoshio Yamaguchi** received the B.E. degree in electronics engineering from Niigata University, Niigata, Japan, in 1976 and the M.E. and Dr. Eng. degrees from Tokyo Institute of Technology, Tokyo, Japan, in 1978 and 1983, respectively. He has been with the Faculty of Engineering, Niigata University during 1978–2019. From 1988 to 1989, he was a Research Associate at the University of Illinois at Chicago, Chicago. His interests are in the field of radar polarimetry, scattering, decomposition and imaging. Dr. Yamaguchi has served as Chair of IEEE Geoscience & Remote Sensing Society Japan Chapter (2002–2003), Chair of URSI-F Japan (2006–2011), and Technical Program Committee Co-Chair of the 2011 IEEE International Geoscience and Remote Sensing Symposium (IGARSS). He is a Fellow of IEEE, and a recipient of 2008 IEEE GRSS Education Award and 2017 IEEE GRSS Distinguished Achievement Award.

**Yuto Minetani** received the B.E. degree from Niigata University in 2018. He was engaged in polarimetric scattering measurement of various trees in anechoic chamber in his Bachelor's research.

**Maito Umemura** received the B.E. degree from Niigata University in 2016. He is a Master student in Niigata University, where he has been engaged in fully polarimetric data processing and utilization. He received Young Scientist Award at the International Conference on SANE, China, Nov. 2018.

**Hiroyoshio Yamada** received the B.E. degree from Hokkaido University in 1988. After earning his Ph.D. in 1993, he joined the Faculty of Engineering, Niigata University, where he is a Professor. He was with NASA-JPL as a visiting scholar on the leave during 2000–2001. His interests include DOA with super resolution techniques such as MUSIC, MIMO radar application, SAR image processing, etc. He has served so many activities of IEICE and IEEE, and received Kiyasu-Zenichi Paper Award and Tutorial Paper Award in 2009, in addition to IEEE APS Tokyo Chapter Award.